

Self-Screened Parton Cascades

Kari J. Eskola

Theory Division, CERN, CH-1211 Geneve23, Switzerland

Berndt Müller

Department of Physics, Duke University, Durham, NC 27708

Xin-Nian Wang

Nuclear Science Division, Lawrence Berkeley Laboratory
Berkeley, CA 94720

Abstract

The high density of scattered partons predicted in nuclear collisions at very high energy makes color screening effects significant. We explain how these screening mechanisms may suppress nonperturbative, soft QCD processes, permitting a consistent calculation of quark-gluon plasma formation within the framework of perturbative QCD. We present results of a model calculation of these effects including predictions for the initial thermalized state for heavy nuclei colliding at RHIC and LHC.

Most recent theoretical predictions for the initial conditions at which a thermalized quark-gluon plasma will be produced at heavy ion colliders are based on the concept of perturbative partonic cascades. The parton cascade model [1] starts from a relativistic transport equation of the form

$$p^\mu \frac{\partial}{\partial x^\mu} F_i(x, p) = C_i(x, p | F_k) \quad i = q, g, \quad (1)$$

where $F_i(x, p)$ denote the phase space distributions of quarks and gluons. The collision terms C_i are obtained in the framework of perturbative QCD from elementary $2 \rightarrow 2$ scattering amplitudes allowing for additional initial- and final state radiation due to scale evolution of the perturbative quanta. To regulate infrared divergences, the parton cascade model requires a momentum cut-off for the $2 \rightarrow 2$ scattering amplitudes (usually $p_T^{\min} = 1.5 - 2 \text{ GeV}/c$) and a virtuality cut-off for time-like branchings ($\mu_0^2 = 0.5 - 1 \text{ GeV}^2/c^2$).

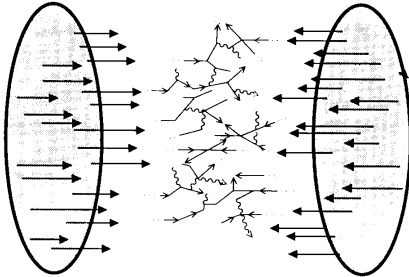


Figure 1: Schematic representation of a nuclear parton cascade.

Numerical simulations of such cascades for heavy nuclei provide a scenario where a dense plasma of gluons and quarks develops in the central rapidity region between the two colliding nuclei shortly after the impact [2]. Detailed studies [3] indicate that the momentum spectrum of partons becomes isotropic and exponential, i.e. practically thermal, at a time $\tau \approx 0.7\Delta z$ in the rest frame of a slab of width Δz at central rapidity. To permit a hydrodynamic description, the width of the slab should exceed the mean free path of a parton. Including color screening effects, one finds that the mean free path of a gluon in a thermalized plasma is $\lambda_f \approx (3\alpha_s T)^{-1}$ where T is the thermal slope of the parton spectrum. For the predicted very high initial values of T (≥ 0.7 GeV) one infers that a thermal hydrodynamic description applies after $\tau_i \approx 0.3$ fm/ c .

The high density of scattered partons in A+A collisions makes it possible to replace the arbitrary infrared cut-off parameters p_T^{min} and μ_0^2 by dynamically calculated medium-induced cut-offs [4]. The dynamical screening of color forces eliminates the need for introduction of the momentum cut-off p_T^{min} , and the suppression of radiative processes provided by the Landau-Pomeranchuk-Migdal effect makes the virtuality cut-off μ_0^2 unnecessary. Note that the viability of this concept crucially depends on the high parton density achieved in nuclear collisions. The dynamical cut-off parameters must lie in the range of applicability of perturbative QCD. Since the density of initially scattered partons grows as $(A_1 A_2)^{1/3} (\ln s)^2$, this condition requires both large nuclei and high collision energy. The calculations indicate that this criterion will be met at RHIC and LHC but not at the presently accessible energies of the SPS and AGS. The framework is also not applicable to pp or $p\bar{p}$ collisions

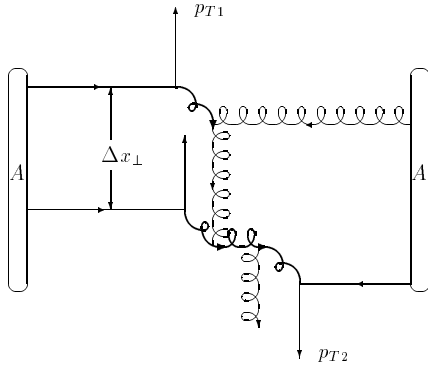


Figure 2: An example of the processes contributing to color screening.

at current energies because the parton density remains too low.

The dynamic screening of parton cascades can be implemented as follows [5]. Consider an example of two hard processes as illustrated in Fig. 2. Let us assume that jets from the first hard scattering are produced at a large angle and carry a high transverse momentum p_{T1} . The interaction point is well localized transversely on a distance of \hbar/p_{T1} . As these two jets travel in the transverse direction, they will experience secondary interactions, which can give rise to many nuclear effects of hard scatterings, e.g. energy loss and Cronin effects. Here the interactions of the produced hard partons with the propagating partons originating from other perturbative scatterings nearby as shown in Fig. 2 are of interest.

A semiclassical estimate of the screening requires that different scattering events can be treated as incoherent. This condition is satisfied if the produced partons, which screen other softer interactions, can be treated as on-shell particles. This requires that the transverse distance Δx_{\perp} between the two scatterings must be larger than the interaction range of the two hard scatterings which are determined by the off-shellness of the exchanged gluons. If this condition is not satisfied, the propagating parton between two scatterings cannot be treated as real and consequently one cannot treat the multiple scatterings as incoherent. We are thus led to consider

$$\tau_f(p_T) = \frac{a\hbar}{p_T} \quad (2)$$

as the formation time of the produced partons in the mid-rapidity region from the hard or semihard scattering after which they can be treated as real (on-shell) particles and can screen other interactions with smaller transverse momentum transfer. The dimensionless coefficient a of order unity parametrizes our uncertainty of the precise formation time.

In the framework of the inside-outside cascade, the incoming nuclei being highly Lorentz-contracted, the primary semihard parton-parton collisions all start at $t = 0$ and the evolving dense system at central rapidity is longitudinally boost invariant. In the space-time evolution of the collision the partons with larger p_T are produced earlier, as implied by (2). These hard partons will then screen production of partons with smaller p_T later in time and space. Since, for fixed p_T , partons with larger rapidities form later in the chosen reference frame, only partons in the same rapidity range are relevant for screening. For the central region around $y = 0$ we consider the screening effect of partons within a unit rapidity interval, $\Delta y = 1$.

We now estimate the static electric screening mass generated by the produced minijets. The number distribution of minijets produced in an AA collision at an impact parameter $b = 0$ can be written as [6]

$$\frac{dN_{AA}}{dp_T^2 dy} = T_{AA}(b) \frac{d\sigma_{\text{jet}}}{dp_T^2 dy}, \quad (3)$$

where $T_{AA}(b)$ is the nuclear overlap function and

$$\frac{d\sigma_{\text{jet}}}{dp_T^2 dy} = K \sum_{ijkl=q,\bar{q}g} \int dy_2 x_1 f_i(x_1, p_T^2) x_2 f_j(x_2, p_T^2) \frac{d\hat{\sigma}^{ij \rightarrow k\ell}}{d\hat{t}}(\hat{s}, \hat{t}, \hat{u}) \quad (4)$$

is the minijet cross section. The hats refer to the kinematical variables of the partonic sub-processes, x_i is the momentum fraction of the initial state parton i , p_T is the transverse momentum, and y is the rapidity of the final state parton. The f_i are the parton distribution functions, and $K = 2$ is a factor accounting for the contribution from higher-order terms in the cross section [7]. For the purpose of screening we treat all the minijets as gluons. This should again be a good approximation, since gluons clearly dominate the minijet production [8].

To obtain an estimate of the average parton number density in the central region at a given time $\tau_f(p_T)$, we divide (3) by the approximate volume

$V = \pi R_A^2 \Delta z \approx \pi R_A^2 \tau_f \Delta y$ of the produced system. Then the static color screening mass becomes [6]

$$\mu_D^2(p_T) \approx \frac{3\alpha_s(p_T^2)}{R_A^2 \tau_f(p_T) \Delta y} 2 \arcsin[\tanh(\Delta y/2)] \int_{p_T}^{\infty} dk_T \frac{dN_{AA}}{dk_T^2 dy} \Big|_{y=0}, \quad (5)$$

assuming that all the quanta with transverse momenta $k_T \geq p_T$ screen the formation of partons at transverse momenta $k_T < p_T$. Only the quanta within the rapidity window Δy are assumed to contribute to the screening mass.

In order to estimate the effect of this screening on the parton scatterings with smaller p_T , we use the computed electric screening mass as a regulator for the divergent \hat{t} - and \hat{u} - channel sub-processes. We will simply make a replacement $\hat{t}(\hat{u}) \rightarrow \hat{t}(\hat{u}) - \mu_D^2$ in the minijet cross sections used in (4). In this way, by feeding the p_T -dependent screening mass back into the equation that defines it, we obtain self-consistent equations for the screening mass and the differential minijet cross section. These equations can be solved numerically by starting at a large p_T with no screening and then integrating down to smaller p_T .

In Fig. 3 we show the screening mass μ_D and the screened one-jet cross section as functions of p_T . In the upper panel the results are shown for the LHC energy $\sqrt{s} = 5.5$ TeV (per nucleon pair) and in the lower panel for the RHIC energy $\sqrt{s} = 200$ GeV. The jet cross sections are based on MRSA structure functions without nuclear shadowing. The figure clearly supports our self-consistent picture of color screening: as the jet cross section grows, the parton medium becomes denser and generates a large screening mass, slowing down the rise of the cross section towards smaller p_T . In this way, the medium of produced minijets regulates the rapid growth of the jet cross section. Finally, at $\mu_D \sim p_T$, the cross section saturates.

To study the lack of sensitivity of the results to details of the uncertainty relation (2), we show curves corresponding to $a = 1$ and $a = 2$. For $A = 200$ collisions at RHIC energy, the screening mass saturates at slightly below 1 GeV, and at 1.5 GeV for collisions at the LHC. Both these values are comfortably within the range of applicability of perturbative QCD, demonstrating that there is no need for an artificial infrared cut-off. The screening of parton scattering by already scattered partons is analogous to the interaction among ladders in the traditional picture of soft hadronic interactions [10]. It would be interesting to rederive our results from this alternative point of view.

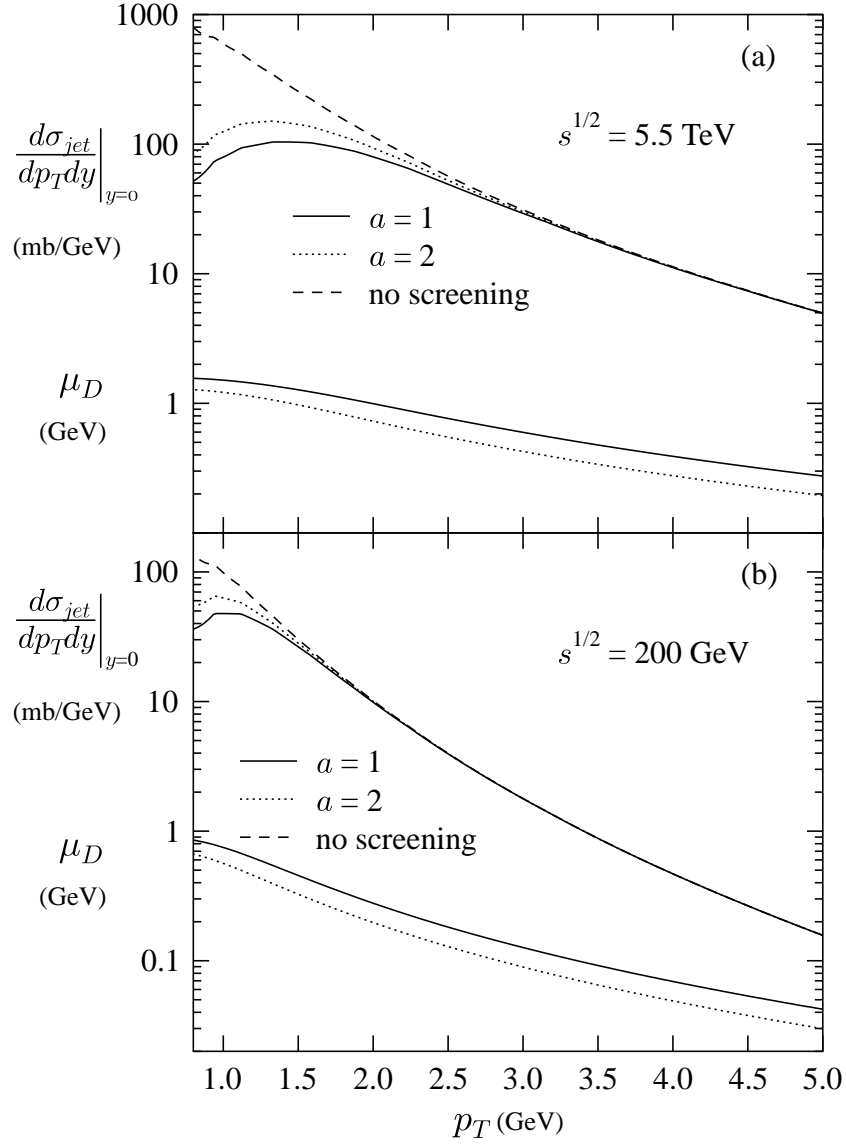


Figure 3: Differential minijet cross section at $y = 0$ and screening mass μ_D as functions of transverse momentum p_T . (a) LHC energy, (b) RHIC energy. Dashed line: without screening; solid and dotted lines: with screening.

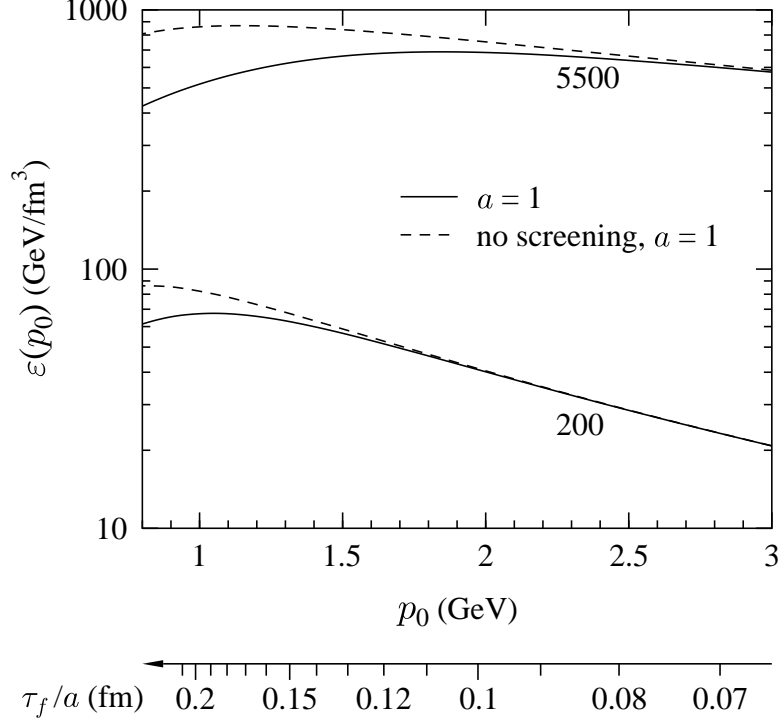


Figure 4: Transverse energy density ϵ of produced minijets as a function of the lowest momentum transfer p_0 or the formation time $\tau_f(p_0)$, respectively. The solid and dashed lines show the estimate with and without color screening.

| $\tau_i = 0.25 \text{ fm}/c$ | RHIC | LHC |
|--|-------|------|
| $\epsilon_i \text{ (GeV/fm}^3\text{)}$ | 61.4 | 425 |
| $T_i \text{ (GeV)}$ | 0.668 | 1.02 |
| $\lambda_q^{(i)}$ | 0.34 | 0.43 |

Table 1: Initial conditions for the hydrodynamical expansion phase at RHIC and LHC. The initial time is taken as $\tau_i = 0.25 \text{ fm}/c$; ϵ_i is the initial transverse energy density, and the effective number of flavors is assumed as $N_f = 2.5$.

In order to study the further evolution of the dense parton plasma created in the first generation of interactions, one can calculate the energy density carried by the scattered partons. The energy density is obtained by dividing the total transverse energy produced by the minijets with momentum transfer p_T exceeding p_0 by the volume corresponding to the formation time $\tau_f(p_0)$:

$$\epsilon(p_0) = \frac{E_T^{AA}(p_0)}{\pi R_A^2 \tau_f(p_0) \Delta y} \equiv \epsilon(\tau_f). \quad (6)$$

The result is shown in Figure 4. As a function of τ_f the energy density first rises as more and more parton scatterings are completed, but later starts to fall on account of the longitudinal expansion when the saturation of minijet production due to color screening sets in.

Since earlier studies [3, 4] have shown that the conditions for a hydrodynamic description of the expansion are satisfied at a time of order $\tau_i = 0.25$ fm/ c , for the energy densities predicted by (6). The full set of initial conditions is listed in Table 1. The initial temperature is predicted to be very high in nuclear collisions both at RHIC and the LHC, but only about one-third of the gluonic phase space is populated by the initial parton interactions. We assumed here that the parton distributions become isotropic due to free-streaming, and no additional transverse energy is produced in the kinetic equilibration. (We emphasize that the assumptions necessary for the conversion of our results into initial conditions for the hydrodynamic evolution introduce considerable uncertainties into the values listed in Table 1. These uncertainties could be eliminated by a microscopic transport calculation of the kinetic equilibration processes.)

Figure 5 shows the evolution of the temperature T , as well as the gluon and quark phase space occupation ratios, λ_g and λ_q , as obtained from a longitudinal hydrodynamical expansion with chemical equilibration [4]. The equilibration only accounts for the processes $gg \rightarrow ggg$ and $gg \rightarrow q\bar{q}$; it may proceed faster if more complex reactions are also included [12]. We have assumed that $\lambda_q^{(i)} = \frac{1}{5}\lambda_g^{(i)}$. The evolution is stopped when the energy density reaches 1.6 GeV/fm³, where the transition to a mixed phase is assumed to occur. The lifetime of the pure plasma is found to be about 4 fm/ c at RHIC and 18 fm/ c at the LHC. For such a long life-time transverse expansion is expected to significantly reduce the plasma life-time at LHC energies and to produce large collective transverse flow [13].

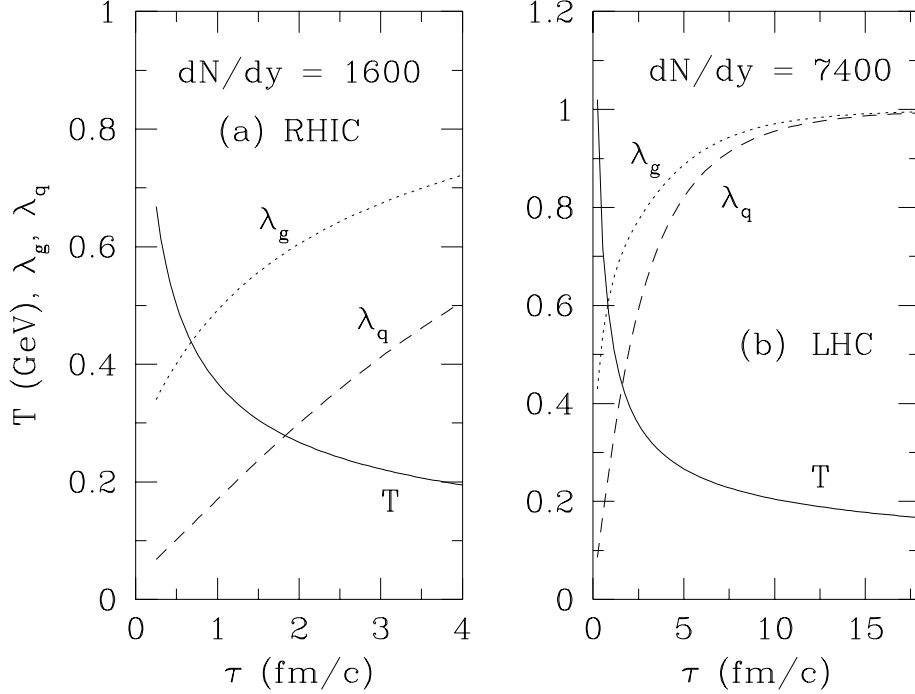


Figure 5: Evolution of the temperature T and parton saturation factors λ_g, λ_q for the initial conditions given in Table 1 in the longitudinal expansion model.

Although many quantitative issues need to be resolved (e.g. the influence of shadowing, the precise formation time, the correct value for Δy) a well-defined picture of a parton cascade in nuclear collisions, which screens its own infrared divergences, is emerging. The screening mass $\mu_D(p_T)$ sets a scale which permits a perturbative description of QCD interactions even in the limit $p_T \rightarrow 0$ as the parton density becomes high. This concept is akin to the picture of random classical color fields proposed in [14] for the small- x gluon structure of large nuclei. It is quite likely that the two approaches can be connected.

Acknowledgements

This work was supported in part by the U.S. Department of Energy (grants DE-FG02-96ER40945 and DE-AC03-76SF00098).

References

- [1] K. Geiger and B. Müller, *Nucl. Phys.* **B369**, 600 (1992).
- [2] K. Geiger, *Phys. Rep.* **258**, 237 (1995).
- [3] K.J. Eskola and X.N. Wang, *Phys. Rev.* **D49**, 1284 (1994).
- [4] T.S. Biró, et al., *Phys. Rev.* **C48**, 1275 (1993).
- [5] K.J. Eskola, B. Müller, and X.N. Wang, *Phys. Lett.* **B374**, 20 (1996).
- [6] T.S. Biró, B. Müller, and X.N. Wang, *Phys. Lett.* **283**, 171 (1992).
- [7] S.D. Ellis, Z. Kunszt and D.E. Soper, *Phys. Rev. Lett.* **62**, 726 (1989); *Phys. Rev.* **D40**, 2188 (1989); *Phys. Rev. Lett.* **69**, 1496 (1992); Z. Kunszt and D.E. Soper, *Phys. Rev.* **D46**, 192 (1992).
- [8] K.J. Eskola, K. Kajantie and P.V. Ruuskanen, *Phys. Lett.* **B332**, 191 (1994).
- [9] B.M. McCoy and T.T. Wu, *Phys. Rev.* **D12**, 546 and 578 (1975).
- [10] S.G. Matinyan and A.G. Sedrakyan, *Sov. J. Nucl. Phys.* **24**, 440 (1976).
- [11] A.D. Martin, W.J. Stirling and R.G. Roberts, *Phys. Rev.* **D51**, 4756 (1995).
- [12] L. Xiong and E.V. Shuryak, *Phys. Rev.* **C49**, 2207 (1994).
- [13] D.K. Srivastava, private communication; B. Kämpfer, private communication.
- [14] L. McLerran and R. Venugopalan, *Phys. Rev.* **D49**, 2233 (1994), *ibid.* **D50** 2225 (1994).